Molecular dynamics study of response of liquid N,N-dimethylformamide to externally applied electric field using a polarizable force field

Citation:
Gao, Weimin, Niu, Haitao, Lin, Tong, Wang, Xungai and Kong, Lingxue 2014, Molecular dynamics study of response of liquid N,N-dimethylformamide to externally applied electric field using a polarizable force field, *Journal of Chemical Physics*, vol. 140, no. 4, Article number: 044501, pp. 1-12.

DOI: http://www.dx.doi.org/10.1063/1.4861893

Molecular dynamics study of response of liquid N,N-dimethylformamide to externally applied electric field using a polarizable force field

Weimin Gao, Haitao Niu, Tong Lin, Xungai Wang, and Lingxue Kong
Institute for Frontier Materials, Deakin University, Waurn Ponds VIC 3216, Australia

(Received 14 October 2013; accepted 30 December 2013; published online 23 January 2014)

The behavior of Liquid N,N-dimethylformamide subjected to a wide range of externally applied electric fields (from 0.001 V/nm to 1 V/nm) has been investigated through molecular dynamics simulation. To approach the objective the AMOEBA polarizable force field was extended to include the interaction of the external electric field with atomic partial charges and the contribution to the atomic polarization. The simulation results were evaluated with quantum mechanical calculations. The results from the present force field for the liquid at normal conditions were compared with the experimental and molecular dynamics results with non-polarizable and other polarizable force fields. The uniform external electric fields of higher than 0.01 V/nm have a significant effect on the structure of the liquid, which exhibits a variation in numerous properties, including molecular polarization, local cluster structure, rotation, alignment, energetics, and bulk thermodynamic and structural properties.
 [http://dx.doi.org/10.1063/1.4861893]

I. INTRODUCTION

N,N-dimethylformamide (DMF) is a commonly used solvent and in applications, such as electrospinning[1] and electric field assisted assembly of nanomaterials,[2,3] it works under an externally applied electric or magnetic field, for example, for electrospinning with needle spinnerets an electric field of about more than 0.01 V/nm at the tip of the needles is generally used. In these processes, the external electric and magnetic fields show significant influence on the intermolecular interaction[4] and, as a results, affect the structure and properties of the liquid. The experimental studies on the influence of external electric field have been limited to the examination of the process and the properties of final products, because of the difficulties in physically measuring the properties of the solution as the external field is presented. For example, the electrostatic properties of a polyvinylidene fluoride (PVDF) and N,N-dimethylformamide electrospinning solution depend on electric field intensity and polarity electric field, whereas the dependence was only presented by the process.[5] With the applied electric field increasing, the diameter of the electrospun fibers gradually decreased.[6] The electrical conductivity and viscosity of DMF solutions were measured under the conditions only without external fields and it was found that DMF induced strong elongation force during the electrospinning process due to its strong polarization.[7]

Computer simulations present a strong capability to analyse the properties of materials under extreme conditions at molecular level, providing a direct route from microscopic details of a specified micro- or nano-system to macroscopic properties of experimental interest. The dependence of the structural and electrical properties of the DMF liquid and its solutions on intermolecular interactions,[8] as well as the relations between the structures and thermodynamic and transport properties, has been widely studied through computer simulation. Most of these studies were under normal conditions. To the best of our knowledge, the intermolecular interaction in liquid DMF under external electric fields and its corresponding structure from molecular dynamics (MD) calculations have not been published yet. However, this is important to understand the behavior of DMF liquid in order to facilitate the better use of external electric fields and design of the nano-device.

The reliability of MD simulation results for liquids depends crucially on the accuracy of the intermolecular potential used. Several all-atom force fields and united-atom force fields have been proposed for liquid DMF, such as the five-site pairwise additive potential (OPLS)[9–11] and the six-site optimized potential (OPLS).[8,12,13] An quantum chemical potential was produced for six interaction centers of liquid DMF by means of *ab initio* calculations where the SCF interaction energies were obtained using the 6-311G(d,p) basis set of the Gaussian 98 program.[14] It should be noted that the five- and six-site OPLS models are based on the experimental conclusion that DMF has no H-bonding possibility in pure liquid phase, even though an energy of 23.45 KJ/mol for hydrogen bond (-HC=O· · ·HC=O) in liquid DMF was calculated from the vaporization enthalpy.[15]

As a primary solvent, DMF is generally mixed with other solutions, such as polystyrene (PS)[16] and polyacrylonitrile (PAN)[17] in electrospinning, or used together with other solvents, such as water, chloroform, and dichloromethane. In this case, hydrogen bonding may be important[18] in the intermolecular interactions and all-atom force fields are required. An all-atom force field, OPLS-AA, was developed for organic molecules and peptides field.[19] For amides, the Lennard-Jones parameters for the CONH group and the charges for the CO unit were taken from OPLS, while the charges on nitrogen and the attached hydrogen were tuned. For DMF molecules, a modification of OPLS-AA was the Lennard-Jones

parameters of carbon on methyl groups. With this modification H-bonds were found between DMF-water,[20,21] however, it was not tested with pure DMF.

The additive force fields with Lennard-Jones potential or other simple functions have shown reasonable accuracy in treating hydrogen bonding under normal conditions. The existence of weak hydrogen bond (–H–C=O· · ·HC=O) in liquid DMF was concluded based on a small positive charge on the hydrogen atom.[9,19] Reliability of the OPLS and OPLS-AA potentials has been tested, showing that the fixed charge force fields can well reproduce many of the structural, thermodynamic, and transport properties of organic molecules, including DMF. However, two key points to be noted during electrospinning are the polarization of molecules and the accumulation of net charges on the molecules. It was found more net charge is accumulated in the molecules in contact with and close to the positive electric pole plate, particularly when high electrostatic field is applied, affecting the spinnability of a PVDF/DMF solution.[5] The fixed atomic point charge force fields show their incapability of representing the electrostatic potential around molecules and of accurately calculating intermolecular forces.

When an external electric field is applied, one first notes the deformation of molecule geometry and local order in the liquid caused by the interaction of the field with the charged atoms. This has been included into most MD packages. Another important response to the externally applied electric field is electric polarization. This response results in molecule deformation through the distortion of the electron density (i.e., the so-called inertia-less polarization) and the displacement of atomic nuclei (i.e., the inertial polarization). In molecular dynamics simulation, this effect has generally been treated by the introduction of an atomic polarization term in response to the redistribution of the electronic density, while the molecule geometry is held frozen.

Various polarization models have been discussed in details[22–24] and the polarizability of atoms and molecules in electric fields has been reported.[25] The most common methods to treat polarization include induced dipoles,[22,26–31] fluctuating charges,[32–35] and Drude oscillators.[36,37]

The polarizabilities of atoms of DMF and other amides can be found in an early publication.[38] The polarizabilities developed by Applequist[38] were used for liquid N-methylacetamide and its aqueous solution by Caldwell and Kollman.[30] The additive model atomic partial charges being the restrained electrostatic potential (RESP) charges were determined using the 6-31G* basis set in Gaussian, and the force field parameters for the additive model were calculated based on the Cornell *et al.* force field.[26] A multicentre multipole expansion (MME) charge distribution over the atoms in molecules and polarizabilities were used in the non-empirical molecular orbital (NEMO) potential and tested with liquid formamide, where the molecular dipole moment and polarizabilities are scaled using rations of the values obtained from the second-order Møller-Plesset (MP2) and the SCF calculations.[39]

A polarizable intermolecular potential function (PIPF) for the simulation of liquid amides was developed by introducing a nonadditive polarization term and the empirical parameters were optimized through Monte Carlo simulations of liquid formamide, *N*-methylacetamide, *N*-methylformamide, and *N*,*N*-dimethylformamide.[40] The induced dipole model (PIPF) was introduced into CHARMMA and its applications to liquid amides, including formamide, N-methylacetamide, and N-methylformamide, and N,N-dimethylformamide was discussed.[41] Comparison of the PIPF and OPLS showed that they predicted similar thermodynamic and structural properties of liquid DMF under normal conditions.[8] Currently there is little study to test its reliability in predicting the physical properties and structure of amides and other molecules under strong external field, although the main advantage of the PIPF model over fixed point charge models, OPLS and OPLS-AA, to be claimed is its ability to provide information about the polarization effects among the molecules in liquid systems.

Another polarizable force field that includes those parameters for various amides is the AMOEBA (Atomic Multipole Optimized Energetics for Biomolecular Applications).[42–46] Comparison of the results for a large set of amino acids under normal conditions showed that the polarizable force fields were more accurate than the fixed charge models.[47] The force field considers the monopole (charge), dipole, and quadrupole moments at each atomic center, and the induced dipole moment at each polarizable atomic site is only submitted to the permanent atomic multipoles. The contribution of externally applied electric field was not included. The AMOEBA force field uses Thole's interactive induction model to treat the polarization effects and a damping scheme is employed for atoms at very short distance to avoid the so-called polarization catastrophe. This approach could be very important with respect to the convergence of the polarization energy, when an extreme high external electric field is imposed on atoms.

In the present work, the AMOEBA force field is extended to include the effect of externally applied electric field; that is, in addition to the bonded and nonbonded terms in the AMOEBA, the interactions of atoms with the external electric field due to atomic partial charge and polarization are also taken into account into the potential. With the modified force field, the thermodynamics properties and structure of pure liquid DMF under a wide range of liquid-external uniform electric fields (0.001 V/nm to 1 V/nm) are investigated. The effect of external electric field on molecular structure and intermolecular interaction is determined by analysing the variations of induced dipole and various energy components. The structure of liquid DMF under different external electric fields is characterized by its local molecule order and molecule orientation.

II. SIMULATION DETAILS

The molecular dynamics simulations are run in the NPT ensemble consisting of 128 DMF molecules placed in a box with periodic boundary conditions at an average temperature of 300 K and 1 atm. To determine the sensitivity of the results to system size, the calculation with 256 DMF molecules at 300 K was performed and yield a value for the total potential energy of each molecule ($-E_{pot}$) that is only 2.74% lower than the results obtained from the 128 molecule system. Further computation to demonstrate the reliability of the

obtained results from the 128 DMF system was not undertaken, however the MD results have provided no evidence to suggest that use of 128 molecules is inadequate. A summary of MD simulations with 64, 128, 256, and 500 DMF molecules at 298 K and 372 K using different force fields[8] shows a low error between the different systems in the prediction of the thermodynamic properties and the bulk properties of DMF liquid, for instance, less than 3% for total potential energy and 0.2% for molar volume, and the error is greatly attributed to the force fields.

The configuration of the liquid phase for property calculation was generated by a NPT dynamics simulation of 2 ns on an initial box with a lower density (0.9 g/cm^3) than the experimental value. In the dynamics simulation, the lengths of the periodic box along all axes (x, y, and z) were allowed to change and the results showed that the obvious shrinkage of the box, or the change of mean liquid density of 0.1 ps, occurred in the first 50 ps. The obtained liquid phase from such a long time (2 ns) NPT calculation then has a comparable density (0.959 ± 0.006 g/cm^3 at 300 K) to the experiments (0.949 g/cm^3[38] and 0.944 g/cm^3[348] at 298 K). Another 1 ns dynamics simulation was performed to calculate the properties of the system without external electric field.

The dynamics simulations were successively performed for the systems under constant uniform external electric fields of 0.001 V/nm, 0.01 V/nm, 0.1 V/nm, and 1 V/nm. In other words, the system resulted from the lower electric field was used as initial liquid structure for the simulation of higher electric field. Each external electric field was imposed for 1.2 ns. The first 1 ns was for the system to reach an equilibrium, the rest to calculate the properties of the system. More detailed information is included in Sec. III.

The constant uniform external electric field, $\boldsymbol{E}_e$, is applied in the z-direction throughout the entire simulation periodic cell. This gives a constant force, $q_i \cdot \boldsymbol{E}_e$, on all the charges in the system, regardless of their position, where q_i is the charge of the ith atom. The atom charges of DMF molecules are from the AMOEBA09 and are fixed; that is, there is no net charge on each molecule. Therefore, electrophoresis does not occur, even for the case of the highest external electric field. The net force on the entire system due to the uniform electric field would be very small.

The polarization of the atom, i, in the system is attributed to the total electric field at its nuclear position, which includes the field, $\boldsymbol{E}_i^d$, generated directly by all other sites, j, and the constant external electric field, $\boldsymbol{E}_e$. The determination of $\boldsymbol{E}_i^d$ has been discussed in details,[43,44] which arises from the permanent multipoles, $\boldsymbol{M}_j$, and the induced dipoles $\boldsymbol{\mu}_j^{ind}$. The multipole is defined at atomic center with a local reference frame formed by neighboring atoms and composed of a point monopole (partial charge), q_{i}, a dipole vector, $d_{\mathrm{i}\alpha}$ ($\alpha = x$, y, and z), and a quadrupole tensor, $Q_{\mathrm{i}\beta\gamma}$ (β, $\gamma = x$, y, and z).[45] The permanent atomic multipoles were derived from *ab initio* quantum mechanics (QM) calculations using the distributed multipole analysis (DMA)[49] and electrostatic potential fitting.[45,50] In brief, the procedure of parameterization mainly includes the optimization of geometry with QM at the HF/6-31G* level, initial QM single-point calculations at the MP2/6-311G** level of theory for electron density matrix and the derivation of initial atomic multipoles from the matrix using the DMA procedure, the electrostatic potential calculation for a gird around each molecule at high-level basis set (MP2/6-311++G(2d, 2p) or MP2/aug-cc-pVTZ), and the optimization of the initial atomic multipole values by fitting to the grid of electrostatic potentials. The electronic polarization is a many-body effect, where the local field produced by the external electric field, permanent multipoles and induced dipoles induces a dipole at each polarizable site, and each induced dipole then updates the field and further polarizes other atoms. This can be treated via Thole's interactive induction model,[51] in which the induced dipole at a site continues to polarize other sites until the induced dipoles at all sites achieve convergence. In the present work, the DIRECT scheme was used for the polarization term. In other words, only the external electric field and the field produced by permanent multipoles were used in the calculation of induced dipoles and the induced dipoles did not involve into the iteration. The comparison with the simulation including the self-consistency computation of induced dipoles (mutual dipole polarization) shows that the DIRECT approach can offer comparable results to the "mutual" calculation, but the computation time is significantly reduced due to the elimination of the self-consistent treatment of polarization effects. In details, the DIRECT approach produced a 4% lower total potential energy and 13% lower polarization energy for the system without external electric field, compared with the mutual dipole polarization.

The quantum mechanics calculations performed in the current work show that when an external electric field of more than 1 V/nm is applied into the system, its contribution could be up to or more than that of $\boldsymbol{E}_i^d$. One could note the convergence of the polarization if such a high field is directly applied into calculation. By default, in order to avoid the "polarization catastrophe" AMOEBA uses a universal polarization damping factor of $a = 0.39$, which was determined based on a fit to water cluster energies[43] and can be used for atoms in small organic molecules and singly charged ions.[46] A stronger damping ($a < 0.39$) has been suggested to better represent the electric field around ions.[44,46,52] In the present work, a lower damping factor ($a = 0.2$) was selected, based on the values for doubly charged cations added to the AMOEBA force field,[53] albeit it was found the performances by using the default factor and the lower one are similar.

The molecular dynamics simulations were performed with a modified version of the open source Tinker software.[54] Particle-mesh Ewald summation method[55,56] was used to treat the long-range electrostatic interactions for both charge and polarization with a real-space cutoff radius of 9.0 Å, a grid size of about 1 Å, and fifth-order B-splines. A cutoff distance of 12 Å was applied for the vdW potential energy interactions. The systems were simulated in the NPT ensemble to ensure the probable change of liquid volume caused by the external electric field. Both the temperature and the pressure were controlled by means of the Berendsen thermostat,[57] whereas a coupling time of 0.1 ps was used for temperature and 1.0 ps for pressure. The motion equations are integrated using the well-known Velocity Verlet algorithm[58] with a 1.0 fs time step.

III. RESULTS AND DISCUSSION

A. Polarization

The presence of an external electric field leads to the distortion of electron density and the electronic polarization provides important information about the interaction of molecules. In the modelling, induced point dipole moment was calculated at each polarizable atomic site according to the electric field. Molecular polarization is based on a Thole-style damped interactive induction model with distributed atomic polarizabilities. The induction scheme can be found in the literature.[44–46] The dipole moments were calculated for all the molecules in the system (Table I). It was found that the dipole moment of the molecules in the condensed phase varies in a wide range, even though there is no external electric field applied. The polarization of a molecule greatly relies on its position and surrounding environment, which is not a surprise considering that in the interactive atomic dipole induction scheme the induced dipole at each polarizable site is submitted to the permanent multipoles and induced dipoles of itself and other atoms, and also considering the difference in the orientation of molecules with respect to the direction of external electric field being applied to the system. The effect of the molecular environment, i.e., the field felt by the molecule, is therefore significant. Experiments have showed that the dipole moment of DMF in benzene solution changes from 3.84 D at 298 K to 4.06 D at 313K and a combined quantum mechanical and molecular mechanical (QM/MM) approach has produced the dipole moments of 3.62 D, 4.05 D, and 5.08 D for DMF in CCl_4, $CHCl_3$, and water, respectively.[40]

There are no direct experimental data that can be used to validate the polarization of DMF molecule under external electric field; comparison of the dipole moments with those from the QM calculations is therefore important. In the present work, a DFT method (B3LYP/6-31+G(*d*,*p*) level of theory) and a high-level *ab initio* method (MP2/aug-cc-pvtz level) were used. The atomic charges fitted to reproduce the molecular electrostatic potential were calculated according to the MK scheme[59,60] to reproduce the dipole moment. The external electric field was imposed in the *x*-direction. The calculations were performed for DMF monomer with Gaussian 09,[61] so that all intramolecular interactions were included in the calculation. As the atomic multipole electrostatic parameters for MD force field have initially been derived from *ab initio* calculations and validated by QM calculation, an excellent agreement between the dipole moments from MD and QM calculations is primarily expected for the system without external electric field after considering that the dipole moment from MD includes the induction from the system. The MD results were well validated by the MP2/aug-cc-pvtz calculations, which produced higher dipole moments than the B3LYP/6-31+G(*d*,*p*) level for DMF under no and low external electric fields and somewhat lower at high external electric fields. The two QM methods produced approximately the same impact strength of external electric field on the dipole moments for all cases. The contribution of local electric field produced by the permanent and induced multipoles to the polarization of a molecule is gradually reduced, as an external electric field is applied, which induces a significant change in the electronic density and electrostatic potentials of the molecule. For this reason and that the variation in dipole moment from the QM calculations mainly presents the contribution of the external electric field, the dipole moments from QM are closer to the average values of the MD results at low external electric field intensities ($\boldsymbol{E_e} < 0.1$ V/nm) and to maximums at high field intensities ($\boldsymbol{E_e} > 0.1$ V/nm).

TABLE I. Dipole moments (unit: Debye) of DMF molecule and the system under the influence of external electric field.

E_e (V/nm)		0.000	0.001	0.010	0.100	1.000
MD (300 K)	System	103.175	111.154	298.360	648.666	744.823
	Mean	4.561	4.600	4.624	4.947	5.439
	Min	3.612	3.619	3.782	3.969	4.308
	Max	5.374	5.439	5.696	5.835	6.382
B3LYP/6-31+G(*d*,*p*)		4.296	...	4.331	4.634	7.763
MP2/aug-cc-pvtz		4.409	...	4.443	4.731	7.727
Exp (gas phase 293 K)		3.820				

Another comparison performed is with the PIPF,[40,41] which calculate dipole moment from the induced moments determined by the defined polarizabilities and the defined permanent charges on the atoms in the liquid, whereas the permanent atomic multipoles in AMOBEA include the monopole (charge), dipole, and quadrupole moments. Gao *et al.*[40] reported a total dipole moment of 4.93 D for liquid DMF by using a previous PIPF force field (PIPF-A). In contrast, the current PIPF gives a total dipole moment of 4.4 D for a liquid phase composed of 256 DMF molecules at 298 K without the presence of external electric field,[41] which is in good agreement with the present QM (MP2/aug-cc-pvtz level) calculation and MD results.

The dipole moment magnitudes of all molecules were averaged and used, along with the minimum and maximum values of the dipole moments, to evaluate the response of polarization of molecules in liquid state to the external electric field (Table I). The difference of them to the dipole moment of DMF monomer should be attribute to the polarization of the molecules, which is due to not only the external electric field but also the permanent multipoles. The mean, minimum, and maximum show the same influence feature of the external electric field on the DMF polarization. Clearly, the effect is great at external electric fields of higher than 0.1 V/nm. The dipole moments of condensed phase are enhanced about 10% by 0.1 V/nm and 20% by 1 V/nm, whereas the average dipole moment in the liquid phase is increased by only 0.9% and 1.4% in 0.001 V/nm and 0.01 V/nm, respectively.

B. Change of liquid structure

1. Pair correlation functions

The change of intermolecular structure of the liquid under external electric field is investigated in terms of the pair correlation functions, $g_{ab}(r)$, which represent the ratio of number density of an atom of molecule *b* at a distance *r* from an atom of molecule *a* to the average number density of the atom.

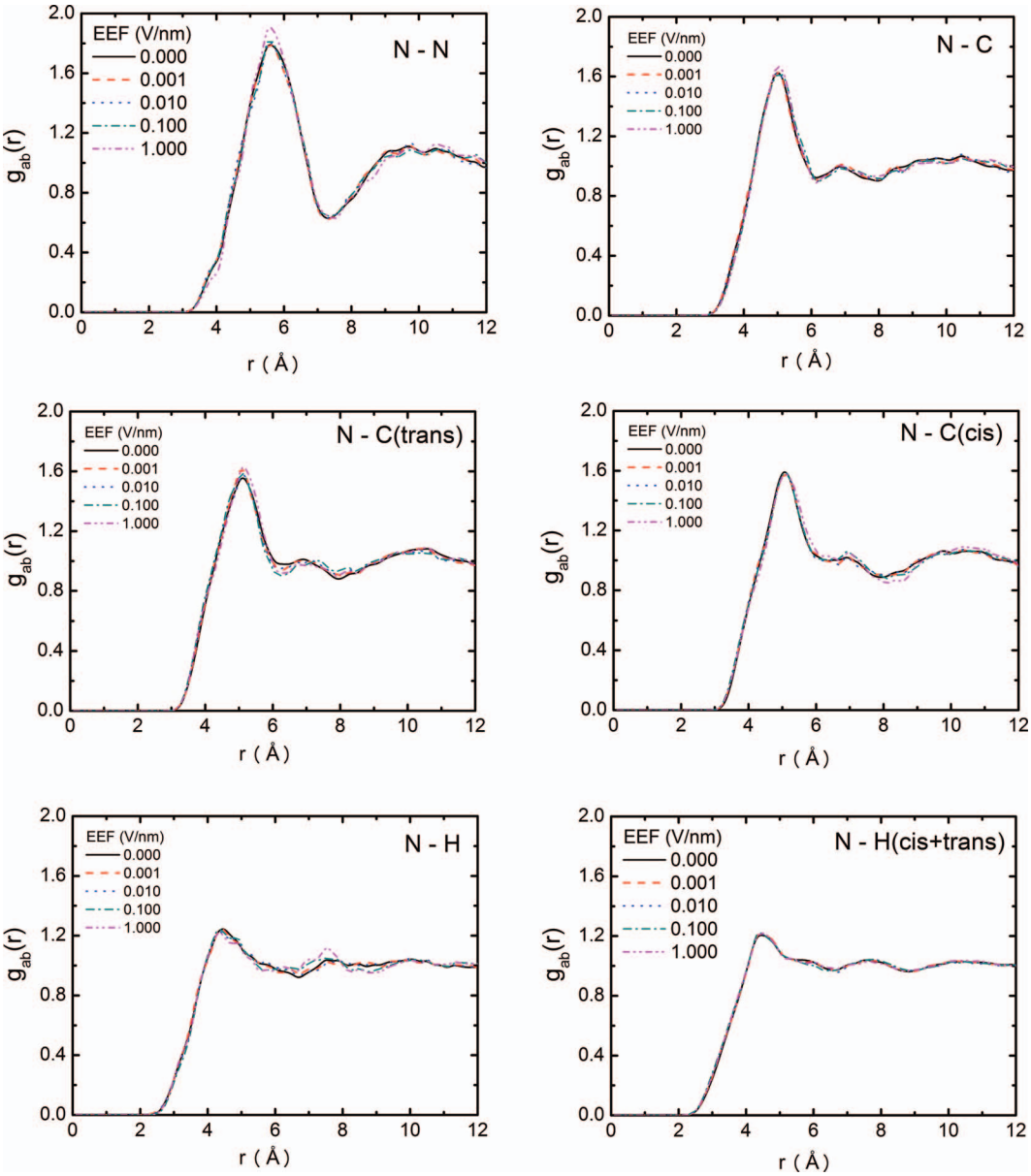

FIG. 1. Site–site (N-X, X denotes each atom in DMF) pair distribution functions of liquid DMF under different electric fields.

The calculation of these functions is performed for atoms to N, atoms to O and C to C with a correlation distance of 16 Å and a resolution of 0.1 Å, as shown in Figs. 1 and 2.

Before examining the effect of the external electric field, the current results for the system at normal conditions were compared with other models, including by comparing the positions and heights of the aforementioned correlation functions to those from the different OPLSs[8,10] and PIPF.[40,41] It was found that there is a good agreement on the characteristics of the depicted functions, considering that the calculations of the redial distribution functions include the intramolecular atoms in the MD simulations of Gao *et al.*[40] It is also noted that the N–N distribution in liquid DMF does not change with temperature at the normal pressure.

It is interesting to find that the distances between the molecule centers and between the methyl groups of a molecule to other molecule centers are not considerably influenced by the external electric field (Fig. 1). The N–N correlation function can be considered as the center of mass (COM-COM) distribution of the system. It is observed that the position of the first peak is at 5.5 Å and does not change with the applied external electric field. The inspection of the data of first peaks for different external electric fields shows that the probability of the N–N distance increases when the external electric field is higher than 0.1 V/nm. An obvious increase can be found for the external electric field of 1.0 V/nm (Fig. 1), which comes with the decrease in the probability of the distances of less than 4.9 Å, especially, the decrease at the distances of less than 4.3 Å. This indicates that the distribution of molecules in the liquid phase becomes more regular when a high-strength uniform external electric field is applied. The integration of the distribution of the first peak produces 4.08 neighbors for systems at normal conditions and with applied external electric fields of 0.001 V/nm and 0.01 V/nm,

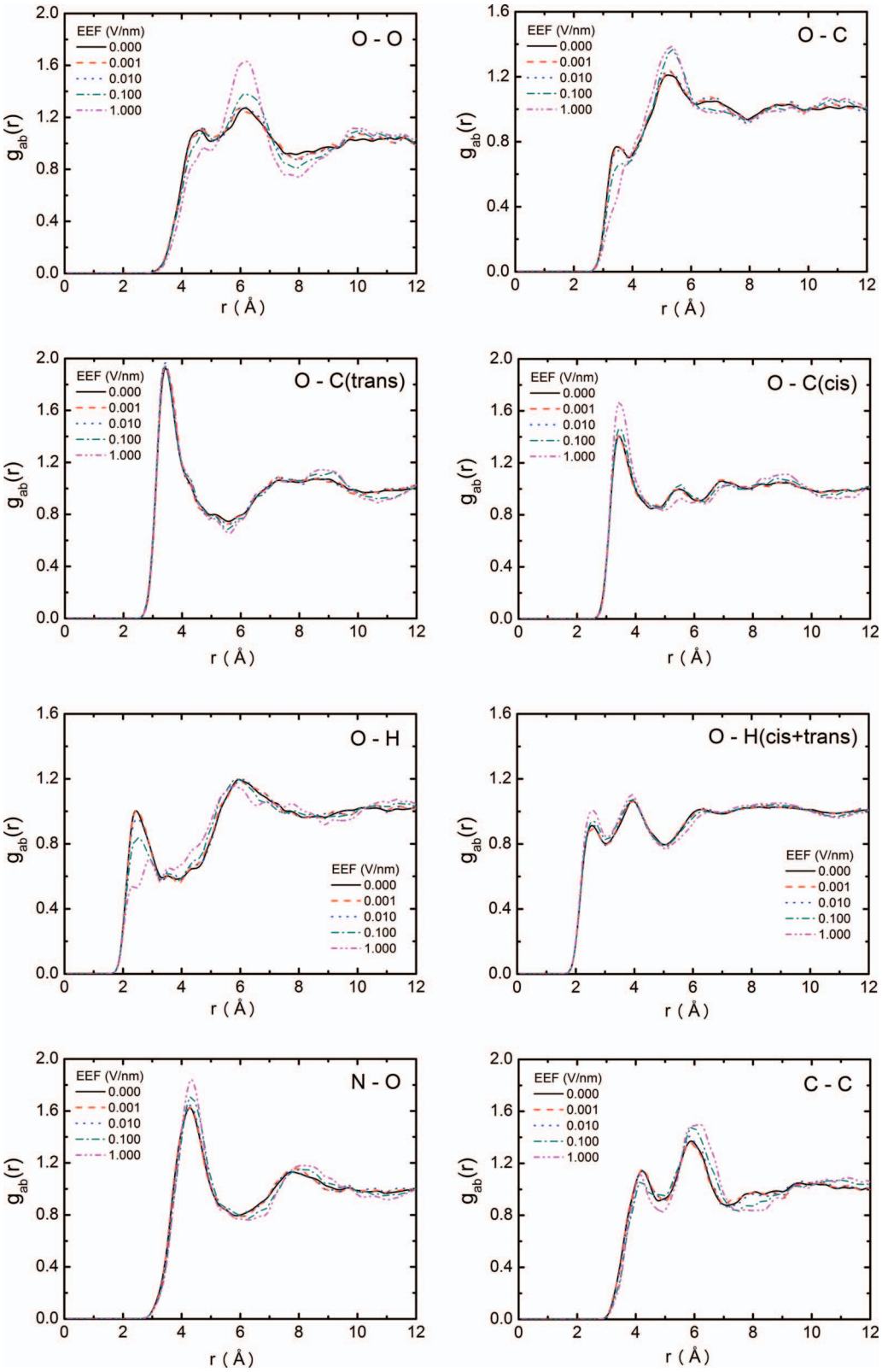

FIG. 2. Site–site (C-C and O-X, X denotes each atom in DMF) pair distribution functions of liquid DMF under different electric fields.

4.09 neighbors for the system with 0.1 V/nm external electric field, and 4.23 neighbors for the system with 1.0 V/nm external electric field. The inspection of the second peak of the N–N distribution shows the peak position shifting to a larger distance as the external electric field is imposed, whereas the location of the overall $g_{ab}(r)$ distribution corresponding to the second peak does not change. This confirms the experimental results[62] and the MD results with other potentials,[8] which show that the DMF molecules tend to form some local orders at an intermolecular distance of about 5.5 Å, and suggests that

this structural feature is not influenced by applying external electric field.

The effect of the external electric field on this liquid structure is mainly presented by the distribution functions of O–O, O–C, O–H, and C–C (Fig. 2), which are the peripheral intermolecular interactions in the liquid, exhibiting a pronounced first peak at a relatively shorter distance followed by a higher second peak at ambient temperature and normal pressure. The application of external electric field reduces the intensity of the first peaks and, on the other hand, increases the second peaks of these site-site distributions. When the external electric field is 1.0 V/nm, the first peaks of the O–O and O–H distribution appear to be very weak and the one of the O–C distribution disappears. By analysing the second peaks of O–O and O–C distribution functions it can be found that both correlations exhibit a similar variation behavior with the application of external electric field, tending to a shape with only one intensive peak at the distance (5.9 Å for O–O and of 5.3 Å for O–C) that is approximately the same as the position of the second peak of their distribution at normal condition ($\boldsymbol{E_e} = 0$). Similar to the effect on weakening the first peaks of O–O and O–C, the external electric field also results in the variation of the number of the interaction of O–H at a short distance (2.5 Å). However, compared to the change of the O–O and O–C distributions, the second peak of the O–H distribution is not intensified, on the contrary, but weakened. Note that the first peaks of O–O, O–C, and O–H distributions are relatively weak in the liquid. Concerning the C–C distribution, the notable change is the broadening of the second peak and the decrease in the distance beyond the second peak. These behaviors indicate that, in addition to order the molecules to the specified direction, the external electric field strengthens the dipolar interactions and reduces the steric effects among neighboring molecules.

The influence of the external electric field on the methyl groups shows a different characteristic (Fig. 2). Note that the C(cis) is the methyl group next to the oxygen atom. It is the nature of this liquid at normal conditions that the first peak of the C(trans)-O function is more intense than the first peaks of the C(cis)-O and the three aforementioned functions (O–O, O–C, and O–H).[8,14] The present work shows that the first peak of the O–C(trans) function does not change with the external electric field. One variation that can be observed in the O–C(trans) function is a new peak appearing at the right-hand side of the plateau between 7.2 and 9.0 Å when the electric field is higher than 0.1 V/nm. On the contrary, the first peak of the O–C(cis) function increases and tends to have a shape same as the shape of the O–C(trans). This can be explained by the strong dipole moment and the tendency to form a coplanar arrangement.

Another notable change is of the O–H distribution. It is found that the results at normal conditions are somewhat different from the MD results with 6-site OPLS[8] and OPLS-AA potentials.[9] They produce first peak height about 1.23–1.30 between 2.6 and 2.9 Å; however, the present MD shows a first peak at a shorter distance (2.5 Å) with a lower maximum height (1.02). With the application of external electric field, the first peak tends to be vanished (Fig. 2). It is also found that the retained second peak is located at a distance approximately the same as the location of the O–O distribution. This is because of the rotation of some molecules along the dipole moment, by which, to form a local liquid structure where the planes of two neighboring molecules are nearly parallel.

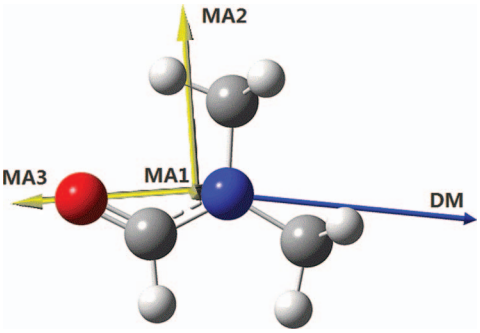

FIG. 3. The principal axes and dipole moment direction of a DMF molecule.

The change of the O–H contacts with the external electric field, together with the O–H(cis+trans) distribution, also confirms the existence of weak hydrogen interactions between the oxygen of a hydroxy group with the hydrogen of other hydroxy groups (–H–O· · ·H–O–) and with the hydrogen of a methyl group (–H–O· · ·CH_3) at normal conditions.[15]

2. Angle distribution density

The effect of external electric field on the structure of the DMF liquid was also confirmed by analysing the orientation and alignment of the molecules (Fig. 3). The principal axes of each molecule were calculated from 100 frames and the first and third components (MA1 and MA3) were used to represent the plane and orientation of the molecules, respectively. To confirm the local order in the liquid, a distribution density was thereafter calculated for both the dihedral angles, θ_{dih}, i.e., the angle between the first principal axes of two neighboring molecules, and the angle between MA3s of molecules and their neighbors, namely, the orientational angles, θ_{oo} (Fig. 4). A distribution density of the molecule orientations with respect to the direction of the external electric field, θ_{oe} (Fig. 5) was also calculated to demonstrate the configuration of molecules under electric field. In the present cases, θ_{oe} is defined by the angle of the vector MA3 to the x-y plane of the simulation systems used, as the uniform external electric field is in the +z direction. Mathematically, the distribution density $p(x)$ is approximated by a set of delta functions of $p_i(x)$ at a value, x_i, of the concerned parameter and has $\int_{x_{min}}^{x_{max}} p(x)\,dx = 1$.

Figures 4 and 5 clearly show that the significant change of the molecule configuration occurs when an external electric field of higher than 0.01 V/nm is imposed, under which the force of the external electric field on some molecules is comparable to the intermolecular interaction, consequently, resulting in the rotation of molecules. Considering the site-site distributions discussed above and the disappearance of the large orientational angles between molecules under the external electric fields of higher than 0.01 V/nm, the rotation

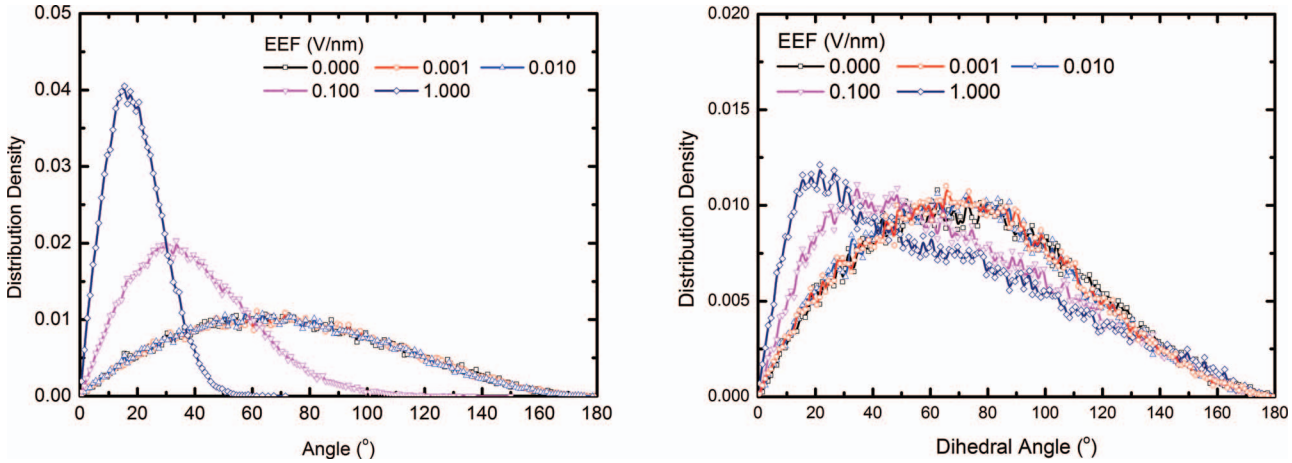

FIG. 4. Distribution densities of angles and dihedral angles between molecules under different external electric fields.

should refer to the molecules in tail-to-tail and head-to-head dimmer configurations and some molecule clusters.

Under the external electric fields of less than 0.01 V/nm, the local structure does not change with the electric field (Fig. 4). Most of the nearest neighbors align with the central molecule at a dihedral angle of about 55°–85° and an orientational angle of about 50°–75°. The integration of the density yields 4 and 3 neighbor molecules for the two molecule orderings ($\theta_{\rm dih} = 55°–85°$ and $\theta_{\rm oo} = 50°–75°$), respectively. Note that the close inspection of the local structure of some molecules reveals that the number of the nearest neighbors of each inspected molecule is in the range of about 11–12.

Having a dihedral angle of near 0° or 180° suggests that the neighboring molecules are in coplanar or parallel-plane arrangement. Only concerning the dihedral angle and orientational angle distribution densities at normal condition in Fig. 4, the inclination of the curves to the angles of 0° indicates the preferential dimmer configurations and the existence of some tail-to-head arrangements ($\theta_{\rm oo}\rightarrow 0°$) for nearly coplanar configurations ($\theta_{\rm dih}\rightarrow 0°$ and 180°) and a few tail-to-tail arrangement where the dipoles of the neighboring molecules in chains are oriented in opposite directions ($\theta_{\rm oo}\rightarrow$ 180°). The tail-to-tail dimmer configuration can be confirmed by the O–H distribution in Fig. 2, in which the H atom of one molecule is in contact with the O atom of another molecule.

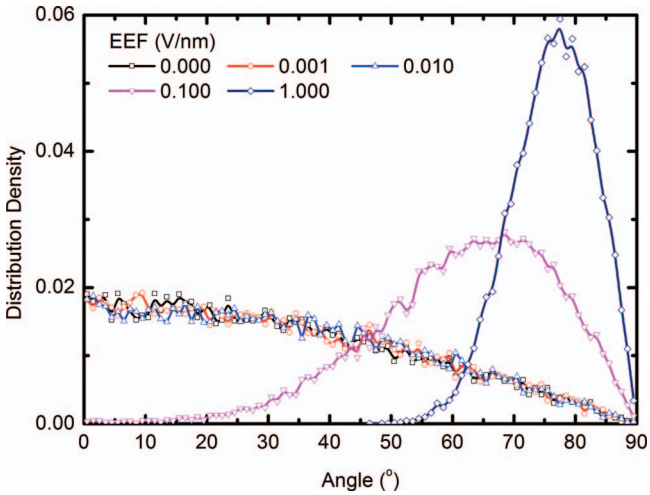

FIG. 5. Distribution density of molecule orientations to the external electric field direction. 0° denotes the molecule orientation normal to the external electric field.

With regards to the minimum energy, the tail-to-tail intermolecular interaction in the liquid, in which the constitutive molecules have a strong dipole moment, cannot be energetically stable enough. This has been discussed with the disappearance of the first peak of the O–H distribution (Fig. 2). This feature is also confirmed from the orientational-angle distribution density with the reduction of the maximum angle of the probable molecular arrangement of 140° under external electric field of 0.1 V/nm to 70° under 1.0 V/nm (Fig. 4).

One important concern in the current work is the strength of external electric field under which the molecules in the liquid start to rotate. The MD results show that the strength should be about 0.01 V/nm (Fig. 5). Closely inspecting the orientation distribution density of molecules under the strength shows that the density for angles between 5° and 20° is reduced. Noting that there is an angle of 170.3° between the molecule orientation and its dipole moment (or 9.7° between the opposite direction of dipole moment and molecule orientation, -DM–MA3) (Fig. 3), it is easily understood the rotation of those molecules that has a dipole moment closely normal to the external electric field, if considering the moment of forces imposed by the electric field. However, under such a low external electric field strength, the number of molecules that can be moved is limited and their rotation would not have an obvious influence on the local molecule arrangement (Figs. 2–4).

There is no doubt that the uniform external electric field has significant effect on the array of dipole molecules. However, the main concern in this study is to what extent the different external electric fields can influence the liquid DMF structure. Figure 5 shows that the molecules nearly normal to the electric field, in specific the molecules of $\theta_{\rm oe} < 20°$, are rotated by the 0.1 V/nm electric field and all molecules in the liquid are well arranged by the 1.0 V/nm electric field. A

TABLE II. Thermodynamic results of liquid DMF under different external electric fields, E_e (V/nm) at 300 K. (T in K; P in atm; ρ in g/cm^3; E_{pot}, E_{eef}, E_{vdw}, E_{pam}, and ΔH_{vap} are in kcal/mol).

E_e	0.000	0.001	0.010	0.100	1.000	0.000 (Exp)	0.000 (MD)
T	298.72	298.85	298.83	299.60	299.55	298	298[a,b,c,d]; 373[e,f]
P	− 85.09	21.57	195.60	88.23	156.48	1	
ρ	0.959	0.950	0.970	0.967	0.976	0.944[g]; 0.949[h]	0.947[a];0.943[b];0.943[c]
E_{pot}	− 8.617	− 8.530	− 9.222	− 11.071	− 33.485	−10.612[h]	−10.696[a]; −11.458 to −10.607[b]; −10.856[e]
E_{eef}	0	− 0.0004	− 0.0717	− 2.237	− 26.063		
E_{vdw}	− 6.135	− 5.860	− 6.043	− 5.947	− 6.404		−6.955[a]; −9.106 to −6.740[b]; 5.473[d]
E_{pam}	− 11.542	− 11.752	− 11.811	− 11.745	− 11.819		−4.05[d]
ΔH_{vap}	11.60	11.68	11.59	11.48	12.61	11.10[g]; 11.36[i]; 12.00[j]	11.36[a]; 11.21[c]; 11.79[d]; 10.49[e]; 10.42[f]

[a]MD results are for a five-site OPLS in the NVE ensemble.[10]
[b]Results are for different six-site OPLS potentials in NPT and NVE ensembles.[8]
[c]Results are for OPLS-AA model in the NPT ensemble.[20]
[d]Results are for PIPF in the NPT ensemble.[40]
[e]MD results are for a five-site OPLS in the NPT ensemble.[9]
[f]Results are for PIPF in the NPT ensemble.[41]
[g]Experimental data are taken from Refs. 48.
[h]Experimental data are taken from Refs. 8.
[i]Experimental data are taken from Refs. 64.
[j]Experimental data are taken from Refs. 41.

maximum distribution density is found at $\theta_{oe} = 77.5^\circ$ for the external electric field of 1 V/nm. Considering the angle between the molecule orientation and the dipole moment (170.3°) and by assuming molecule dipole moments tending to be parallel with the direction of the external electric field, it can be estimated that the angle with the maximum density is 87.2°. One could expect that θ_{oe} is 90° by supposing that the dipole moments are parallel to the direction of the electric field. However, when considering the intermolecular interaction and the existence of molecules that are greatly angled to the electric field direction, it is understood the nature of $\theta_{oe} < 90^\circ$. Therefore, the angle of 87.2° and the angle of 78.2° for the 0.1 V/nm electric field (calculated from the θ_{oe} with the maximum density plus the angle of -DM–MA3) do have physical meaning and quantitatively represent the effect of the corresponding external electric fields.

In addition to the quantification of the molecule rotation to the opposite direction of the electric field, the rotation of neighboring molecules to each other is also characterized. Figure 4 shows that the angles between the orientations of neighboring molecules, with respect to the maximum probability, are 15.5° and 33.5° under 1 V/nm and 0.1 V/nm electric fields, respectively. This confirms that, because of the intermolecular interactions, the most of dipole moments are nonparallel to the electric field direction.

Under an external electric field the neighboring molecules also rotate on their axes (MA3) to form a local molecule order where most of the molecules are nearly parallel, as demonstrated from the variation of the distribution density of dihedral angles shown in Fig. 4. The shift of the peak from an angle close to 90° to an angle close to 0° indicates a rotation from near-perpendicular to near-parallel configurations. Note that the most neighboring molecules also face approximately the same direction.

One may also expect the distribution of dipole moments of the molecules in the liquid. However, the dipole moment of each molecule changes, in both its magnitude and its direction, with not only the applied external electric field but also the molecule polarization achieved based on the point dipole moments at each polarizable atomic site of the molecule. Furthermore, the polarization of each atom is dependent on its neighbors and self-dependence. By taking all of the above considerations into account, it can be anticipated that, compared to the principal axes, the analysis of the liquid structure based on the dipole moments would be very complex and not immediately apparent.

C. Thermodynamic properties

The temperature, T, the pressure, P, and the density, ρ, of the system, the mean potential energy of each molecule in liquid phase, E_{pot}, the energy due to the external electric field, E_{eef}, the van der Waals, E_{vdw}, and atomic multipoles, E_{pam}, to the total energy of each molecule were calculated for different external electric fields, E_e (Table II). The van der Waals (vdW) intramolecular, $E_{vdw\text{-}intra}$, and vdW intermolecular interaction, $E_{vdw\text{-}inter}$, of each molecule in the box were calculated and their average together with the minimum and maximum values are given in Table III.

The heat of vaporization, ΔH_{vap} was calculated from the total intermolecular potential energy of the liquid, $E_{inter}(l)$, the intramolecular energies of the liquid, $E_{intra}(l)$, and the gaseous phase, $E_{intra}(g)$, and the PV component by Eq. (1). $E_{inter}(l)$ was computed over all the intermolecular energies at a cutoff of 12.5 Å. $E_{intra}(g)$ was determined by excluding the binding

TABLE III. Intra- and inter-molecular van der Waals energies (kcal/mol).

E_e (V/nm)		0.000	0.001	0.010	0.100	1.000
$E_{vdw\text{-}inter}$	Mean	− 11.122	− 11.012	− 11.140	− 10.888	− 11.452
	Min	− 14.617	− 14.713	− 14.798	− 14.437	− 15.111
	Max	− 8.128	− 6.520	− 7.582	− 6.614	− 7.806
$E_{vdw\text{-}intra}$	Mean	4.987	5.153	5.098	4.940	5.048
	Min	2.133	2.626	2.831	2.225	2.329
	Max	7.954	7.862	8.775	7.836	9.267

energy obtained by QM calculation at the MP2/aug-cc-pvtz level[63] from the AMOEBA energy of a gas phase dimer[46]:

$$\Delta H_{vap} = E_{intra}(g) - E_{inter}(l) - E_{intra}(l) + RT. \quad (1)$$

The present MD results were first compared to the experiments and MD results from OPLS and PIPF force fields before analysing the effect of external electric field. The comparison was only performed for the liquid phase under normal condition ($E_e = 0$), as there is no experimental and calculated data for the influence of external electric field on the thermodynamic properties of the liquid. Although the electric field plays an essential role in the concerned processes, more attentions have been paid to the process response and the effect on the product properties, because of the difficulty in the observation of the thermodynamic properties of the liquid being under an external electric field.

The comparison clearly indicates the strengths and weaknesses of the AMOEBA in describing the thermodynamics of this liquid. When compared to the experimental data, it slightly underestimates the potential energy of the DMF liquid. This feature is also found after carefully analysing the results of its application to other liquid amides and some small molecules.[46] It has been claimed that the overall performance of the AMOEBA on the predicting properties of 30 small molecules is slightly better than traditional fixed charge force fields.[44] The comparison in the present work, however, shows that the united-atom and all-atom OPLS models and PIPF mode can produce a potential energy for DMF liquid that is in good agreement with the experimental results and some OPLS models give a better prediction on the density and vaporization of this liquid. However, it should be kept in mind that the results are, to certain extent, dependent on the size of box and computational conditions used in the modelling and this has been widely demonstrated.

Table II clearly shows the influence of external electric field on the liquid properties. It becomes important when it is up to 0.01 V/nm, at which the contribution of external electric field to the total energy increases to 0.8% and an obvious increase in density and decrease in the potential energy and vaporization can be found. This is excellent agreement with the pair correlation functions and the angle distribution densities.

It can be seen that the permanent atomic multipole component (E_{pam}) is the major contribution compared to that of other components in all cases except the external electric field of 1.0 V/nm. Specially, the ratio of E_{pam}/E_{vdw} is approximately 2. Considering this including the contribution of charges in the AMOEBA force field, the ratio is first compared with these from the OPLS[8] and PIPF[40] models. However, it is found that, on the contrary, these models yield much lower electrostatic energies (E_{ele}) than van der Waals parts (E_{vdw}), in specific, the ratio (E_{ele}/E_{vdw}) is about 0.5 and 0.8 for most OPLS models and PIPF, respectively. If considering that the atomic multipole component (E_{pam}) also includes the contribution of the dipole and quadrupole moments of the atoms that have high polarizabilities, this inconsistency is understandable. Furthermore, the AMOEBA, OPLS, and PIPF use different functions for the pairwise additive van der Waals interaction, the former adopts the buffered 14-7 functional form,[65] whereas the latter two use the Lennard-Jones 6–12 function. The difference in the results of the two functions has been discussed.[44]

By comparing the atomic multipole energies from different external electric field, it is clearly seen that the energy increases with the strength of electric field. This is also attributed to the change of dipole and quadrupole moments with the external electric field.

The mean vdW energies over the system show a complex effect of the external electric field. As shown in Figs. 4 and 5, the molecules in the liquid arrange in a wide range of orientation. The external electric field influences not only the intermolecular interaction but also the molecule structure (Table III). The present QM calculations demonstrate the change of the DMF structure with the applied external electric field. For examples, when the electric field is imposed along the dipole moment of the molecule, the N–C bond decreases from 1.357 Å at 0 V/nm, 1.357 Å at 0.01 V/nm, 1.355 Å 0.1 at V/nm, to 1.333 Å at 1 V/nm; the C–O bond increases from 1.223 Å, 1.224 Å, 1.226 Å, to 1.249 Å; the C(cis)-N-C(trans) angle from 117.77°, 117.76°, 117.62°, to 116.03°; the N–C–O angle from 125.59°, 125.61°, 125.77°, to 1257.40° Therefore, when the changes of molecule structure and the local order of molecules are taken into account, the complexity of the influence can be expected. Although the mean values of $E_{vdw\text{-}inter}$ and $E_{vdw\text{-}intra}$ somewhat represent this feature, the minimum and maximum values of both interactions more clearly show the dependence of local molecule interaction and atomic vdW interaction of specified molecules on the external electric field.

IV. CONCLUSIONS

When an external electric field is applied to a molecular cluster and a condensed phase, it not only generates an electrostatic force on each charged atom but also leads to distortion of electron density, which in turn changes the local electric field and then the electrostatic force on the points that can feel the change. In the present study, we extend the AMOEBA polarizable force field to include these interactions. With this extended force field, the effect of externally applied uniform electric fields with different strengths on the structure of liquid N,N-dimethylformamide has been studied through NPT molecular dynamics simulations performed on a high-performance computing (HPC) system. The molecular polarization, intermolecular interaction, local molecule order, and energies as well as the thermodynamic and structural properties of the liquid in response to the external electric field were analysed and compared with experimental results and other molecular dynamics simulations with united-atom and all-atom OPLS and PIPF force fields. Quantum mechanics calculations at B3LYP/6-31+G(*d*,*p*) and MP2/aug-cc-pvtz levels were also performed to evaluate the molecular dynamics simulation.

The results of the simulations for a wide range of external electric field strengths (from 0 V/nm to 1 V/nm) show that the external electric fields of higher than 0.01 V/nm have a significant effect on the structure of liquid N,N-dimethylformamide. It is mainly represented by the peripheral intermolecular interactions in the liquid, i.e., the weakening of O–O, O–C, O–H,

and C–C interactions and the enhancement of O–C(cis) and O–H(trans and cis) interactions. The effect is first attributed to the rotation of the molecules with an angle of about 10° with respect to the direction of applied external electric field. Under a uniform external electric field, in addition to the rotation to the electric field, a major response of liquid phase is the motion of molecules tending to form a local structure where molecules are near-parallel to one another. Nevertheless, the distances between the molecule centers and between the methyl groups of a molecule to other molecule centers are not considerably changed under the external electric fields of less than 0.1 V/nm. The molecules would be well aligned when a uniform electric field of more than 1 V/nm is applied. The relative orientation and alignment of neighboring molecules are very sensitive to the electric field strength, and they can be well represented by the distribution densities of the molecule orientations, the dihedral angles and the orientational angles between molecules and their neighbors, which are defined in this paper.

The external electric field induces minor geometrical deformations in the molecule, in specific, the N–C and C–O bonds and the C(cis)–N–C(trans) and N–C–O angles. The dipole moments of the molecules in the liquid phase greatly depend on their position and surrounding environment and vary in a wide range, even though at a high external electric field (more than 0.1 V/nm) at which the influence on the molecule polarization is great, for instance, the mean dipole moment is increased about 10% and 20% by 0.1 V/nm and 1 V/nm external electric fields, respectively. Owing to the molecules in the liquid phase have different orientations with respect to the direction of the uniform external electric field, the influence of the electric field on the intermolecular interaction for the entire liquid phase is very complex. The weak hydrogen bonds, H–C=O· · ·H–C=O, are eliminated to a certain degree corresponding with the strength of the external electric field, while the interaction between the oxygen with the hydrogen of methyl group (H–C=O· · ·H_3C) are slightly enhanced.

ACKNOWLEDGMENTS

Support from Australian Research Council through a Linkage Project (No. LP100100422) is gratefully acknowledged. Most of the computations were performed with the facilities of the Victorian Partnership for Advanced Computing (VPAC).

[1] S. Basu, A. K. Agrawal, and M. Jassal, J. Appl. Polym. Sci. **122**, 856 (2011).
[2] Z. Nie, D. Fava, E. Kumacheva, S. Zou, G. C. Walker, and M. Rubinstein, Nat. Mater. **6**, 609 (2007).
[3] M. Senthil Kumar, T. H. Kim, S. H. Lee, S. M. Song, J. W. Yang, K. S. Nahm, and E. K. Suh, Chem. Phys. Lett. **383**, 235 (2004).
[4] Y. Zhao, K. Dong, X. Liu, S. Zhang, J. Zhu, and J. Wang, Mol. Simul. **38**, 172 (2012).
[5] C. Yang, Z. Jia, Z. Guan, and L. Wang, J. Power Sources **189**, 716 (2009).
[6] K. H. Lee, H. Y. Kim, Y. M. La, D. R. Lee, and N. H. Sung, J. Polym. Sci., Part B: Polym. Phys. **40**, 2259 (2002).
[7] L. Lu, D. Wu, M. Zhang, and W. Zhou, Ind. Eng. Chem. Res. **51**, 3682 (2012).
[8] M. Chalaris and J. Samios, J. Chem. Phys. **112**, 8581 (2000).
[9] W. L. Jorgensen and C. J. Swenson, J. Am. Chem. Soc. **107**, 569 (1985).
[10] J. W. Essex and W. L. Jorgensen, J. Phys. Chem. **99**, 17956 (1995).
[11] H. Torii, M. G. Giorgini, and M. Musso, J. Phys. Chem. B **116**, 353 (2012).
[12] M. Chalaris and J. Samios, J. Mol. Liq. **78**, 201 (1998).
[13] M. Chalaris, A. Koufou, and J. Samios, J. Mol. Liq. **101**, 69 (2002).
[14] Y. P. Puhovski, L. P. Safonova, and B. M. Rode, J. Mol. Liq. **103–104**, 15 (2003).
[15] A. K. Baev, *Specific Intermolecular Interactions of Organic Compounds* (Springer-Verlag, Berlin, 2012), p. 29.
[16] C. L. Pai, M. C. Boyce, and G. C. Rutledge, Macromolecules **42**, 2102 (2009).
[17] J. C. Chen and I. R. Harrison, Carbon **40**, 25 (2002).
[18] M. Umadevi and R. R. Poornima, Spectrochim. Acta, Part A **73**, 815 (2009).
[19] W. L. Jorgensen, D. S. Maxwell, and J. Tirado-Rives, J. Am. Chem. Soc. **118**, 11225 (1996).
[20] Y. Lei, H. Li, H. Pan, and S. Han, J. Phys. Chem. A **107**, 1574 (2003).
[21] G.-Z. Jia, K.-M. Huang, L.-J. Yang, and X.-Q. Yang, Int. J. Mol. Sci. **10**, 1590 (2009).
[22] S. Rick and S. Stuart, in *Reviews in Computational Chemistry*, edited by K. Lipkowitz, and D. Boyd (John Wiley & Sons, Inc., 2002), Vol. 18, p. 89.
[23] P. E. M. Lopes, B. Roux, and J. A. D. MacKerell, Theor. Chem. Acc. **124**, 11 (2009).
[24] A. D. Mackerell, J. Comput. Chem. **25**, 1584 (2004).
[25] G. Maroulis, in *Atoms, Molecules, and Clusters in Electric Fields: Theoretical Approaches to the Calculation of Electric Polarizability*, Computational, Numerical, and Mathematical Methods in Sciences and Engineering Vol. 1 (Imperial College Press, London, 2006), pp. 1–32.
[26] W. D. Cornell, P. Cieplak, C. I. Bayly, I. R. Gould, K. M. Merz, D. M. Ferguson, D. C. Spellmeyer, T. Fox, J. W. Caldwell, and P. A. Kollman, J. Am. Chem. Soc. **117**, 5179 (1995).
[27] L. X. Dang, J. Phys. Chem. B **102**, 620 (1998).
[28] D. N. Bernardo, Y. Ding, K. Krogh-Jespersen, and R. M. Levy, J. Phys. Chem. **98**, 4180 (1994).
[29] A. Wallqvist and B. J. Berne, Chem. Phys. Lett. **117**, 214 (1985).
[30] J. W. Caldwell and P. A. Kollman, J. Phys. Chem. **99**, 6208 (1995).
[31] M. Sprik, J. Phys. Chem. **95**, 2283 (1991).
[32] R. A. Bryce, M. A. Vincent, N. O. J. Malcolm, I. H. Hillier, and N. A. Burton, J. Chem. Phys. **109**, 3077 (1998).
[33] S. W. Rick and B. J. Berne, J. Am. Chem. Soc. **118**, 672 (1996).
[34] S. W. Rick, S. J. Stuart, and B. J. Berne, J. Chem. Phys. **101**, 6141 (1994).
[35] S. Patel, A. D. Mackerell, Jr., and C. L. Brooks III, J. Comput. Chem. **25**, 1504 (2004).
[36] L. R. Pratt, Mol. Phys. **40**, 347 (1980).
[37] B. G. Dick, Jr., and A. W. Overhauser, Phys. Rev. **112**, 90 (1958).
[38] J. Applequist, J. R. Carl, and K.-K. Fung, J. Am. Chem. Soc. **94**, 2952 (1972).
[39] S. Brdarski, P.-O. Åstrand, and G. Karlström, Theor. Chem. Acc. **105**, 7 (2000).
[40] J. Gao, J. J. Pavelites, and D. Habibollazadeh, J. Phys. Chem. **100**, 2689 (1996).
[41] W. Xie, J. Pu, A. D. Mackerell, and J. Gao, J. Chem. Theory Comput. **3**, 1878 (2007).
[42] J. W. Ponder and D. Case, Adv. Protein Chem. **66**, 27 (2003).
[43] P. Ren and J. W. Ponder, J. Phys. Chem. B **107**, 5933 (2003).
[44] J. W. Ponder, C. Wu, P. Ren, V. S. Pande, J. D. Chodera, M. J. Schnieders, I. Haque, D. L. Mobley, D. S. Lambrecht, R. A. DiStasio, M. Head-Gordon, G. N. I. Clark, M. E. Johnson, and T. Head-Gordon, J. Phys. Chem. B **114**, 2549 (2010).
[45] Y. Shi, Z. Xia, J. Zhang, R. Best, C. Wu, J. W. Ponder, and P. Ren, J. Chem. Theory Comput. **9**, 4046 (2013).
[46] P. Ren, C. Wu, and J. W. Ponder, J. Chem. Theory Comput. **7**, 3143 (2011).
[47] J. Wang, P. Cieplak, J. Li, J. Wang, Q. Cai, M. Hsieh, H. Lei, R. Luo, and Y. Duan, J. Phys. Chem. B **115**, 3100 (2011).
[48] D. R. Lide, *CRC Handbook of Chemistry and Physics* (CRC Press, Boca Raton, FL, 2000), p. 1 CD.
[49] A. J. Stone and M. Alderton, Mol. Phys. **56**, 1047 (1985).
[50] J. C. Wu, G. Chattree, and P. Ren, Theor. Chem. Acc. **131**, 1138 (2012).
[51] B. T. Thole, Chem. Phys. **59**, 341 (1981).
[52] D. Jiao, C. King, A. Grossfield, T. A. Darden, and P. Ren, J. Phys. Chem. B **110**, 18553 (2006).

[53]D. Semrouni, W. C. Isley, C. Clavaguéra, J.-P. Dognon, C. J. Cramer, and L. Gagliardi, J. Chem. Theory Comput. **9**, 3062 (2013).
[54]J. W. Ponder and F. M. Richards, J. Comput. Chem. **8**, 1016 (1987).
[55]U. Essmann, L. Perera, M. L. Berkowitz, T. Darden, H. Lee, and L. G. Pedersen, J. Chem. Phys. **103**, 8577 (1995).
[56]T. Darden, D. York, and L. Pedersen, J. Chem. Phys. **98**, 10089 (1993).
[57]H. J. C. Berendsen, J. P. M. Postma, W. F. v. Gunsteren, A. DiNola, and J. R. Haak, J. Chem. Phys. **81**, 3684 (1984).
[58]L. Verlet, Phys. Rev. **159**, 98 (1967).
[59]U. C. Singh and P. A. Kollman, J. Comput. Chem. **5**, 129 (1984).
[60]B. H. Besler, K. M. Merz, and P. A. Kollman, J. Comput. Chem. **11**, 431 (1990).
[61]M. J. Frisch, G. W. Trucks, H. B. Schlegel *et al.*, Gaussian 09, Revision D.01 (Gaussian, Inc., Wallingford, CT, 2009).
[62]R. Konrat and H. Sterk, J. Phys. Chem. **94**, 1291 (1990).
[63]R. Vargas, J. Garza, R. A. Friesner, H. Stern, B. P. Hay, and D. A. Dixon, J. Phys. Chem. A **105**, 4963 (2001).
[64]G. Mamantov and A. I. Popov, *Chemistry of Nonaqueous Solutions: Current Progress* (VCH, New York, NY, 1994), p. 307.
[65]T. A. Halgren, J. Am. Chem. Soc. **114**, 7827 (1992).